Pergamon

Journal of Structural Geology, Vol. 16, No. 3, pp. 403 to 418, 1994

0191-8141/94 $06.00+0.00

Grain boundary sliding and development of grain boundary openings in experimentally deformed octachloropropane

J.-H. REE*

Department of Geological Sciences, State University of New York at Albany, 1400 Washington Avenue, Albany, NY 12222, U.S.A.

(*Received* 18 *June* 1991; *accepted in revised form* 26 *April* 1993)

Abstract—*In situ* observations of grain boundary sliding and associated accommodation mechanisms in experimentally pure- and simple-sheared octachloropropane at 75–85% of its absolute melting temperature and at strain rates of 10^{-5}–10^{-6} s^{-1} are discussed. Discontinuities in the strain, rotation and/or translation components of deformation across the grain boundary induce grain boundary sliding. The influence of crystallographic orientation of grains on grain boundary sliding is so strong that grains unfavorably oriented for basal slip contribute to deformation mainly by grain boundary sliding. Grain boundary diffusion and intragranular plastic deformation are observed to accommodate grain boundary sliding. Grain boundary diffusion also causes grain boundary migration (Types II and III) that is different from conventional grain boundary migration (Type I) in being non-conservative, and in the details of boundary movement with respect to material points within grains. Grain boundary openings filled with fluid (octachloropropane vapor) are strongly associated with grain boundary sliding. Openings develop preferentially along grain boundaries at low angles to the shortening direction. Once openings grow, they are closed by thrusting of sliding grains and by diffusion in faster strain-rate experiments, and entirely by diffusion in slower strain-rate experiments. An approximately steady openings ratio of 0.5–3% of the sample volume persists without the development of any large-scale fracture. All grain boundary openings disappear during static readjustment of the microstructure after deformation.

INTRODUCTION

IN PLASTIC flow of polycrystalline materials above about 30–50% of their absolute melting temperature there are two types of deformation mechanisms, lattice mechanisms and boundary mechanisms. The distinction is based on whether the individual processes are independent of or dependent on the presence of grain boundaries (Langdon 1975, 1981, Langdon & Vastava 1982). Two important processes of boundary mechanisms are grain boundary sliding and diffusional creep. However it is difficult to find unequivocal evidence for grain boundary sliding and diffusional creep in naturally or experimentally deformed rocks (Schmid *et al.* 1977, Schmid 1982, Behrmann 1985).

The aim of this paper is to present detailed, *in situ* observations of grain boundary sliding and associated accommodation processes in an experimentally deformed rock analog material. The creation and healing of grain boundary openings associated with grain boundary sliding, their geological implications, three types of grain boundary migration, and the recognition of grain boundary sliding and openings in rocks will also be discussed.

In the geological literature, there have been several terms for grain boundary openings produced during plastic flow. *Grain boundary void* was used most frequently (White 1977, White & White 1981, Hall 1984, Behrmann 1985, Ree 1988, Knipe 1989). However void may not be a good term for grain boundary openings that are believed to contain some fluid, as in naturally deformed rocks and in the experiments described here (White & White 1981, Behrmann 1985, Urai personal communication 1988). *Intergranular cavity* was used by Davidson *et al.* (unpublished abstract, Leeds Conference 1989), but this term is avoided in this paper for the same reason. *Intergranular microfracture* (Cox & Etheridge 1989) and *grain boundary microcrack* (Drury & Urai 1990) have also been used. Since grain boundary opening in plastic flow does not necessarily involve fracturing or cracking (e.g. Stowell *et al.* 1984, Chokshi & Langdon 1987), the term *grain boundary opening* is favored in this paper.

GRAIN BOUNDARY SLIDING AND ITS ACCOMMODATION

Grain boundary sliding is a process in which grains slide past each other along, or in a zone immediately adjacent to, their common boundary (Langdon & Vastava 1982). Adams & Murray (1962) first observed grain boundary sliding in experimentally deformed bicrystals of NaCl and MgO, where offset of marker lines preinscribed across the grain boundary occurred. *In situ* observation of grain boundary sliding in a Zn–Al alloy was made by Naziri *et al.* (1973, 1975), using electron microscopy. They inferred grain boundary sliding from the observation of grain neighbor switching during deformation. Considering the extensive grain boundary migration in their photographs, however, neighbor switching alone does not provide convincing evidence of grain boundary sliding, because neighbor switching can be achieved by grain boundary migration alone (Means & Ree 1990, Bons & Urai 1992).

*Present address: Department of Geology, Kangwon National University, Chunchon, Kangwon-do 200-701, Korea.

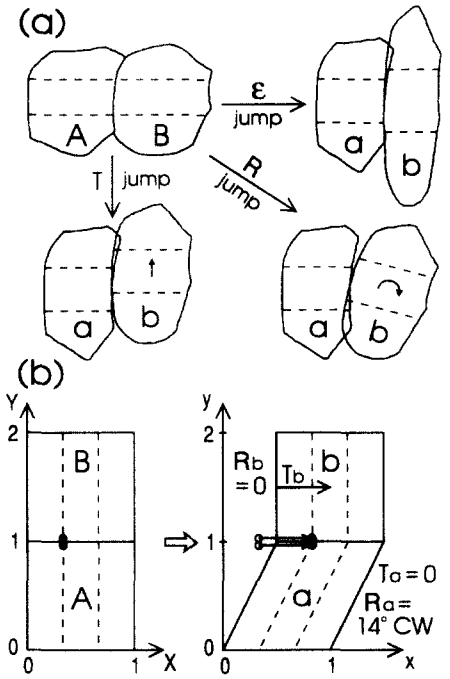

Fig. 1. (a) Schematic diagram illustrating why grain boundary sliding occurs. Top left: two grains (A and B) in the undeformed state with two straight marker lines (broken lines). Top right: grain boundary sliding due to a strain jump. Bottom right: grain boundary sliding due to a rotation jump. Bottom left: grain boundary sliding due to a translation jump. (b) Schematic diagram to show that strain, rotation or translation jump does not necessarily cause grain boundary sliding. Grain A is dextrally sheared ($\gamma = 0.5$) while grain B is rigidly translated, inducing a strain jump (from a maximum principal strain of about 0.28 to zero strain), a rotation jump (from about 14°CW rotation of the principal strain direction to zero rotation), and a translation jump (from $T_a = 0$ to $T_b = 0.5$) across the boundary from grain a to b. However, grain boundary sliding does not occur since material particles at the boundary (black dots) are displaced into the same positions by each domainal deformation of the grains.

Grain boundary sliding is a probable process in plastic flow of polycrystals if there is deformation incompatibility among grains and if the necessary accommodation mechanisms for grain boundary sliding can operate. Figure 1(a) shows, in a schematic way, three possible situations for grain boundary sliding, where there is a strain jump, rotation jump or translation jump between grains. However strain, rotation or translation jumps do not necessarily produce grain boundary sliding if material at the contact or boundary is maintained in coherent contact by suitably matched deformations of the two grains (see also Means & Jessell 1986) (Fig. 1b).

Obviously some simultaneous accommodation mechanisms must operate to avoid the types of overlaps between sliding grains as shown in Fig. 1, and between a sliding grain and a blocking grain in front of the sliding grain. Many authors have suggested that openings also should be avoided to maintain a coherency between grains (e.g. Crossman & Ashby 1975, Edward & Ashby 1979). However, complete coherency at grain boundaries is not a rigid requirement in grain boundary sliding (Langdon 1970). Therefore I will restrict the accommodation problem to overlaps since only overlaps are physically impossible. Accommodation mechanisms suggested in the literature of metallurgy and materials science are elastic distortion, dislocation movement and diffusion.

Elastic distortion can accommodate grain boundary sliding by deforming sliding and blocking grains elastically. With this accommodation mechanism the sliding displacement must be small relative to the length of the sliding surface, and it may be recoverable when the stress is removed (Raj & Ashby 1971).

Dislocation movement can accommodate grain boundary sliding by forming a localized deformation zone adjacent to the triple junction within a blocking grain ('triple-point fold', Fig. 2a) or at ledges of the grain boundary between sliding grains (Gifkins 1976, Etheridge & Wilkie 1979, Langdon & Vastava 1982, Zeuch 1984, Hashimoto *et al.* 1987), by deforming a whole blocking grain with slip and twinning (Crossman & Ashby 1975) (Fig. 2b), or by climb and glide within the grain boundary mantle (Gifkins 1976) (Fig. 2c).

Diffusional accommodation occurs by transport of material either along the grain boundaries or through the lattices of grains (Raj & Ashby 1971, Ashby & Verrall 1973) (Fig. 2d). Grain boundary sliding accommodated by this mechanism is considered as a normal part of diffusional creep, since diffusional creep should be accompanied by grain boundary sliding to maintain coherency between deforming grains (Raj & Ashby 1971, Ashby & Verrall 1973, Langdon 1975, Gifkins 1976, Speight 1976, Langdon & Vastava 1982). Grain boundary sliding and diffusional creep are, therefore, considered to be coupled and mutually accommodating (Poirier 1985).

EXPERIMENTAL RESULTS

Thin sheets of octachloropropane (C_3Cl_8, hereafter called OCP) mixed with marker particles (1000-grit silicon carbide) were deformed in a press mounted on the stage of an optical microscope for *in situ* observation

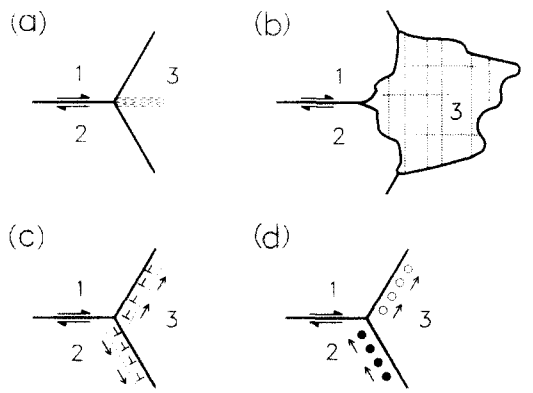

Fig. 2. Accommodation mechanisms of grain boundary sliding. (a) Localized deformation adjacent to the triple junction within a blocking grain (grain 3). (b) Intragranular plastic deformation of a whole grain. Dotted lines represent deformation bands. (c) Dislocation glide and climb in the grain mantle (after Gifkins 1976). Dotted lines represent boundaries between grain mantle and core. Movements of dislocations in the mantle are schematically shown. (d) Diffusion along grain boundaries around the triple junction (after Gifkins 1976).

and recording of deformation processes. This technique of 'synkinematic microscopy' is explained in greater detail by Means (1989).

Samples before deformation were annealed at 50–60°C in an oven for more than 5 days to provide relatively coarse and equiaxed grains. Before running an experiment, a sample was again heated statically on the deformation apparatus at the deformation temperature for 2–12 h. Then samples were deformed under pure-shear or simple-shear geometry. Strain rate was about 10^{-5} s^{-1} except in one experiment, TO-202, which was done at a shear strain rate of about 10^{-6} s^{-1}. Temperature during deformation was 60–100°C corresponding to 75–85%, respectively, of the absolute melting temperature of OCP. The conditions of the experiments described in this paper are presented in Table 1.

The bulk strain of each sample was determined by averaging strains indicated by five to 10 sets of three marker particles with average distance of about 1 mm between the marker particles in a set. The bulk strains of smaller areas in samples were calculated in the same way as the bulk strain of a sample but using marker particles around the specific areas. The intragranular strain of individual grains was measured from displacements of one–five sets of three widely spaced marker particles within a grain, and it is not necessarily homogeneous within the grain. Other techniques measuring *c*-axis, grain size and grain-shape foliation are described by Ree (1991).

In the following subsections three simple-sheared samples will be described in detail since they have a larger population of marker particles than other samples, which allows a more complete description of grain boundary sliding and its accommodation. Sample TO-110, which was deformed mainly by intragranular deformation (Ree 1991), shows evidences of grain boundary sliding induced by translation and strain jumps. In sample TO-105, grain boundary sliding due to translation and rotation jumps, and its accommodation by intragranular plastic deformation, will be illustrated. Although experimental conditions of TO-105 were almost the same as TO-110 except the initial *c*-axis orientation (see below), its deformation behavior was strikingly different from TO-110, with an extensive development of grain boundary openings (see Figs. 7a–h) and the greater component of grain boundary sliding in its total deformation. In experiment TO-202 which was done at the slowest strain rate in this paper, extensive grain boundary openings also developed. Clear evidence of grain boundary sliding induced by translation jump, diffusional accommodation and diffusion-related grain boundary migration will be presented in this sample.

In preparation of an OCP sample before deformation, some preferred orientation of *c*-axes is always introduced due to the pressing of the sample between two glass slides perpendicular to the plane of observation to obtain a desired sample thickness (≅30–40 μm) and some preferred extrusion along the deformation window during sample pressing. The usual shape of *c*-axis preferred orientation before deformation is a broad, single girdle normal to the direction of shear in simple shearing experiment as in TO-110 and TO-202 (see Fig. 12f). But in sample TO-105 the initial *c*-axis orientation forms a girdle at a low angle to the shear direction for some unknown reason (see Fig. 9a).

Experiment TO-110

In this experiment, the initial average grain area of about 1×10^{-2} mm^2 increases by about 23% after a bulk shear strain of 0.5. From this strain onwards, the average grain area of 1.2×10^{-2} mm^2 becomes steady to the end of the deformation (Ree 1991). Intragranular strain is heterogeneous with the stretch ratio (S_1/S_3) of individual grains ranging from 1.3 to 5.5 at a total bulk shear strain of 1.3. Progressive increase in the bulk area, determined by 10 sets of three marker particles, occurs during the deformation and it is about 15% at the end of the deformation.

Figure 3 shows a portion of the sample where eight material lines drawn approximately perpendicular to the shear direction, with the help of marker particles, provide a clue to grain boundary sliding induced by a translation jump. At a bulk shear strain of 0.1, tiny grain boundary openings occur between grains 93 and 95, and between grains 76 and 96 (Fig. 3a). Their size is about 2 μm (or about 0.02 the average grain diameter) wide and 20–30 μm (or about 0.2–0.3 the average grain diameter) long. After an additional local bulk shear strain of 1.2, all material lines are stretched and rotated (Fig. 3b). All but two material lines passing through grains 95 and 96 remain more or less parallel to each other without any offset. These two lines show offset of about 75 μm across the boundary between grains 95 and 96. Grain 95 is not strained much. Its basal slip plane is almost perpendicular to the shortening direction S_3, assuming this direction is at about 45° to the shear direction. Grain 95 thus is a

Table 1. Experimental conditions

Experiment	Deformation type	Strain rate* (s^{-1})	Total strain	Temperature (°C)	Duration of deformation (h)
TO-88	Pure shear	2.2×10^{-5}	−0.5 (ε_3)	70	6.25
TO-89	Simple shear	7.8×10^{-5}	1.8 (γ)	70	6.42
TO-100	Pure shear	2.3×10^{-5}	−0.5 (ε_3)	100	6.17
TO-105	Simple shear	5.3×10^{-5}	1.8 (γ)	80	9.50
TO-110	Simple shear	3.8×10^{-5}	1.3 (γ)	80	9.50
TO-202	Simple shear	9.6×10^{-7}	0.2 (γ)	60	58.00

*Axial strain rate for pure-shear experiments and shear strain rate for simple-shear experiments.

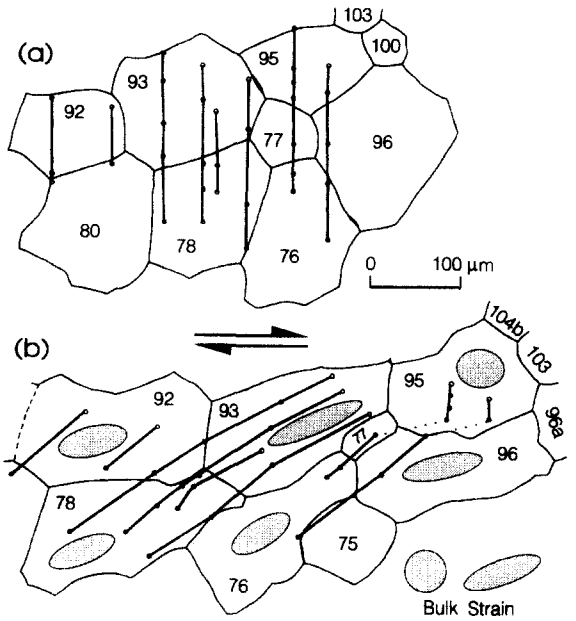

Fig. 3. Maps of the central area of OCP sample TO-110 (a) at bulk shear strain γ of the whole sample = 0.1 and (b) after deformation (γ = 1.3). Thick lines represent material lines drawn using marker particles. The bulk strain ellipse of the mapped area is shown in the bottom right of (b). Intragranular strain ellipses are also drawn for most of the grains.

'hard' grain with the basal plane unfavorably oriented for slip (Ree 1990). Grain 96 on the other hand is strained almost the same as the bulk strain ellipse for the whole group of grains. Without grain boundary sliding this strain difference should have been represented by a kink-like feature of the material lines without any offset. The offset of the lines running through the two grains implies grain boundary sliding in which grain 95 is translated more or less rigidly past grain 96.

Figure 4(a) shows the evolution of the boundary between grain 95 and a grain left behind (grain 93). Here the grain boundary opening noted earlier would increase its size as grain 95 slides to the right with respect to grain 96 if enough material were not added into the opening by diffusional influx, or if grain 93 were not translated together with grain 95. As seen in Fig. 4(a) the grain boundary opening does not grow. Instead it is almost closed at the end of the deformation. However, the area occupied by four marker particles across the grain boundary increases continuously with the deformation (Fig. 4a). The total increase in area is about 50% at the end of the deformation. Diffusional influx of material probably accounts for this area increase.

An accommodation with the grain blocking the sliding grain 95 should involve the diffusional efflux of the material, a zone of plastic high strain along the boundary or plastic deformation of the blocking grain, unless the blocking grain overlaps with the sliding grain or is translated together with the sliding grain. Initially the blocking grain is grain 100 and later it becomes grain 96a after grain 100 has been consumed by grain 96 (Fig. 3). In the boundary between grains 95 and 100, a tiny opening also develops during the deformation, but it closes at the end of the deformation when the boundary becomes at a high angle to the shortening direction (Fig. 4b). Unfortunately there are not enough marker particles to measure the area change adjacent to this boundary. The development of the grain boundary opening between grains 95 and 100 may involve an area increase around the boundary, suggesting translation of grain 100 to the right at least as fast as grain 95. Grain sliding along the boundary approximately parallel to the bulk shear direction as described above was found at eight sites in this sample, mainly around hard grains. The amount of offset is usually 70–80 μm, or 0.6–0.7 the average grain diameter.

Grain boundary sliding is also expected along boundaries that are not parallel to the bulk shear direction if there exists a strain or rotation jump between grains. Figure 5 shows the c-axis orientations and marker particle trajectories of grains 76 and 78 for a period of deformation during which a bulk shear strain of about 0.7 has accumulated from the stage in Fig. 3(a). The trend of the basal slip plane in grain 76 was inclined toward the shear direction at the beginning of the deformation, and the c-axis of grain 76 rotated clockwise

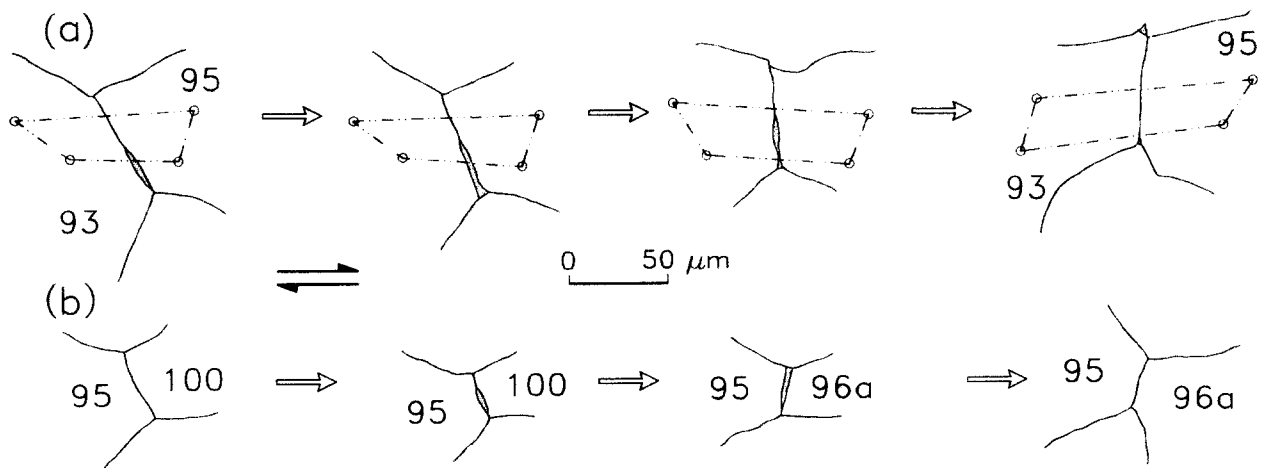

Fig. 4. Evolution of boundaries between (a) grains 93 and 95 and (b) between grains 95 and 100 in sample TO-110. Grain 100 later becomes grain 96a after consumed by grain 96. Shaded area represents a grain boundary opening. Marker particles are indicated by small circles.

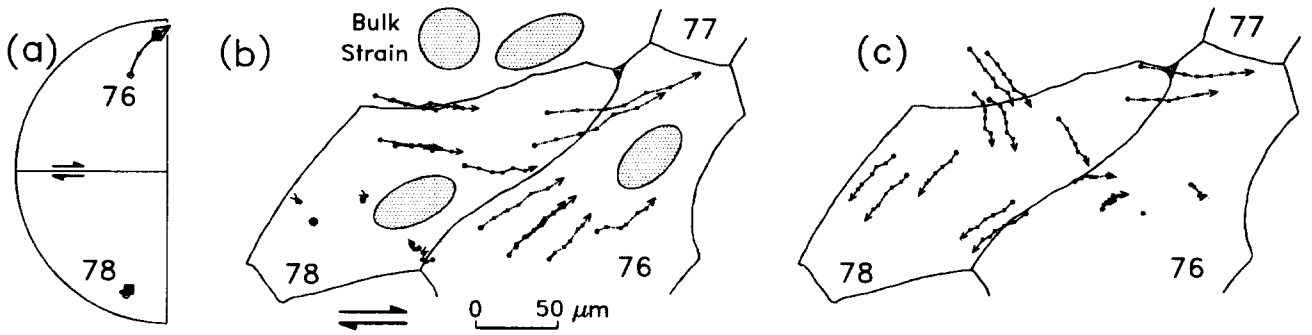

Fig. 5. (a) Western half-circle of a lower-hemisphere stereographic projection showing *c*-axis trajectories of grains 76 and 78 in sample TO-110. Open circle and tip of arrow represent *c*-axis before and after deformation, respectively. Solid square indicates *c*-axis at the stage of (b). *c*-axis of grain 78 remains in almost the same position after the stage of (b). (b) Map of the two grains at a bulk shear strain of the area shown in Fig. 3 ≅ 0.7. Marker particle trajectories are drawn using marker particles that remain in the same grain, relative to a fixed particle in grain 78 (solid circle). Initial position of a marker particle is represented by an open circle. The tip of an arrow indicates a marker particle position at a bulk shear strain $\gamma \cong 0.7$. Particle positions in-between are represented by crosses. (c) Marker particle trajectories at the same stage as in (b) but relative to a fixed particle in grain 76 (solid circle).

by about 25° after an interval of deformation in Fig. 5. On the other hand, the trend of the basal slip plane in grain 78 inclined against the shear direction at the beginning of the deformation, and the *c*-axis of grain 78 stayed in almost the same position (Fig. 5a). The trajectories of marker particles in grain 78 relative to a fixed point within this grain show displacements approximately parallel to the trend of its basal slip plane, suggesting basal slip is the primary deformation mechanism in grain 78 (Fig. 5b). The trajectories of marker particles in grain 76 relative to a fixed point within this grain also tend to show displacements parallel to the trend of its basal plane (Fig. 5c), but whether basal slip predominates or not is unclear because of the rotation of its *c*-axis. The deformation of these two grains with different displacement fields results in different maximum stretch (S_1) directions (44° vs 25° CCW from the shear direction) and in different rotations of S_1 (25° vs 18° CW), even though the stretch ratios in the two grains (1.9 vs 2.1) do not differ greatly (Fig. 5b).

In Fig. 6(a) a material line was drawn almost perpendicular to the boundary between the two grains using marker particles within the grains. This material line is approximately parallel to the trend of the basal slip plane in grain 78 and at a high angle to that of the basal plane in grain 76. As expected with basal slip, the segment of the material line in grain 78 does not change its length and orientation with increasing deformation. If other slip systems had been associated with basal slip, the material line initially parallel to the basal plane should have changed at least its length. On the other hand, the segment of the material line in grain 76 becomes shortened and rotated, producing an offset of the line of about 80 μm at the end of the deformation (Fig. 6d). Therefore it is believed that this offset represents grain boundary sliding induced by a strain jump or difference in the maximum stretch direction and a rotation jump between grains 76 and 78.

Experiment TO-105

In this simple-shear experiment (Fig. 7), the average grain area of about 1.3×10^{-2} mm^2 before the deformation increases by 53% to 2.0×10^{-2} mm^2 during the accumulation of a bulk shear strain of about 0.9. Then, after some decrease in average grain area, the sample maintains a steady average grain area at about 1.8×10^{-2} mm^2 to the end of the deformation. There is almost no change in the bulk area during the deformation.

Figure 9 shows *c*-axis fabric diagram before and after deformation and *c*-axis reorientation trajectories of some grains in the central area of the sample. During dextral simple shear, the intragranular plastic deformation of grains is accompanied by clockwise rotation of

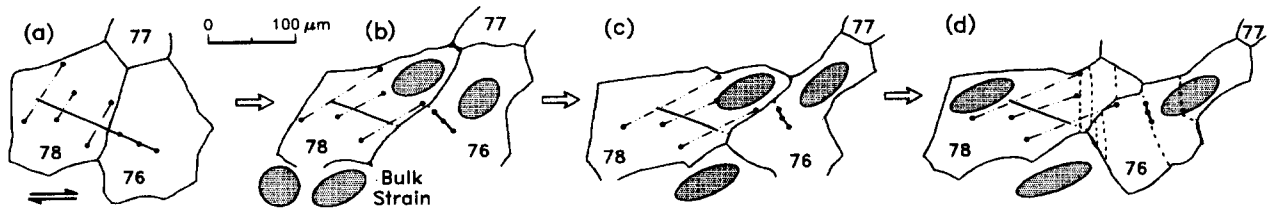

Fig. 6. Offset of a marker line crossing the boundary grains 76 and 78 in sample TO-110. (a) Bulk shear strain of the sample ≅ 0.1. Additional bulk shear strains of the area in Fig. 3 from the stage (a) are about (b) 0.6, (c) 0.9 and (d) 1.2. Broken lines in (d) represent subgrain boundaries. The segment of the marker line in grain 78 was drawn by interpolating the positions of marker particles, and the segment in grain 76 was drawn by connecting marker particles. Not all marker particles used to calculate strains are shown.

c-axes (Fig. 9c). When the c-axes of most grains are in positions unfavorable for basal slip, grain boundary openings begin to occur in association with relatively rigid translation and rotation of most grains in the sample (Figs. 7c and 9c). Grain boundary openings develop preferentially along boundaries at low angles to the shortening direction, inclining against the bulk shear direction or the direction of relative displacement of the upper part of the shearing sample. Their widths range from about 2 μm up to 40 μm with a typical width of about 5 μm or about 0.04 the average grain diameter. Their lengths, ranging from about 15 to 200 μm, are mostly 50 μm or about 0.4 the average grain diameter. After an initial increase, grain boundary openings occupy 1–2% of the sample area, and remain constant at that value until the deformation stops. Further details of the evolution of these grain boundary openings will be discussed later.

An example of grain boundary sliding resulting from translation jump is illustrated in Fig. 10 which shows grain boundary maps, marker particle trajectories and c-axis trajectories for three grains in the sample during an interval of the deformation. The three grains are deformed mainly by intragranular plastic deformation and their c-axes rotate clockwise by 10–30° during bulk shear strain of about 0.9 (Figs. 10a & b). As the basal planes of the grains approach an orientation unfavorable for slip, the deformation becomes dominated by grain boundary sliding, and openings begin to develop preferentially along boundaries at a low angle to the shortening direction (Figs. 10c–f). With an additional shear strain of about 0.4 from the stage of Fig. 10(a), a material line defined by marker particles across the grains 22 and 11 shows an offset of about 100 μm or about 60% of the average grain diameter of the sample (Fig. 10e). The maps of marker particle trajectories in Figs. 10(d) & (f) indicate that this grain boundary sliding results mainly from a translation jump between grains 11 and 22.

Across the grain boundaries under possible compression due to the grain boundary sliding, such as the boundary between grains 11 and 3a, and the boundary adjacent to the junction of grains 3a, 3b and 22 (Fig. 10e), the areas occupied by each four marker particles show only a few percent decrease from the stage of Fig. 10(c) to (e). This implies that diffusional accommodation is not significant at these sites. Note also that the grains are not perfectly rigid but are internally strained during grain boundary sliding. As indicated by the intragranular strain ellipses, however, the magnitudes of intragranular strain are lower than that of the bulk strain (Figs. 10c & e). Grain 3 is more strongly strained than the other grains and shows rotational recrystallization resulting in grain-size reduction. This suggests that grain boundary sliding is accommodated mainly by intragranular plastic deformation at these compressional areas. At boundaries possibly under extension, grain boundary sliding causes openings to occur that could serve as sink sites of diffusion. Indeed, some grains show overgrowths into the grain boundary openings, suggesting diffusional influx into these sites (Figs. 7e & f). The source sites of diffusion are not clear from the marker particle population and scale.

Figure 11 shows grain boundary sliding due to a rotation jump between grains 25a and 26. As the sample is deformed, intragranular plastic deformation and clockwise c-axis rotation are followed by the formation of grain boundary openings, as in the previous example. After a bulk shear strain of about 1.2 (Fig. 11a), the two grains deform in significantly different manners. The trajectories of marker particles within grain 25a (Figs. 11d & f) and very weak intragranular deformation implied by the incremental, intragranular strain ellipses (Figs. 11c & e) indicate that grain 25a is deformed mainly by clockwise rigid-body rotation. The c-axis of grain 25a also rotates clockwise by about 20° (Fig. 11b), and its grain-size increases with the consumption of adjacent grains during this deformation interval. In contrast, the intragranular strain of grain 26 is stronger even than the bulk strain of the local area comprising these two grains. Grain 26 also shows grain-size reduction by rotational recrystallization and grain boundary migration (Figs. 11a–c), and only a small rotation of its c-axis (Fig. 11b). Grain boundary sliding associated with the more or less rigid-body rotation of grain 25a is evidenced by the offset of a marker line drawn almost perpendicular to the boundary between the two grains. The healing and shape change of openings at the northeast and southwest boundaries of grain 25a, and the creation of openings at the boundary between grains 25a and 26, are associated with this grain boundary sliding (Fig. 11e). The reason why the two grains behave differently, even though the orientations of their c-axes relative to the shear direction are similar at the beginning of the deformation interval described above, is unclear. Perhaps the stress field is highly heterogeneous in that area.

Experiment TO-202

Experiment TO-202 is the slowest simple-shearing experiment described in this paper ($\dot{\gamma} \cong 9.6 \times 10^{-7}\,s^{-1}$, Table 1). A total shear strain of about 0.2 was imposed over about 58 h, at 60°C. The initial average grain area of about 2.2×10^{-2} mm^2 increases gradually to 2.9×10^{-2} mm^2 at the end of the deformation. The change in the bulk area does not occur during the deformation. The c-axis fabric diagram before deformation shows a broad girdle normal to the direction of shear as usually observed in other simple shearing experiments (Fig. 12f).

As in experiment TO-105, extensive grain boundary openings associated with grain boundary sliding develop. They develop, however, at a lower shear strain than in TO-105 (less than 0.1). Their ratio is about 1% of the sample area at $\gamma \cong 0.1$. Offset of a marker particle line and marker particle trajectories in Fig. 12 indicate that a translation jump is mainly responsible for the grain boundary sliding between grains 4 and 6 (Figs. 12a–c). Across a boundary possibly under compression due to the grain boundary sliding, the area occupied by four marker particles decreases by about 15% during an

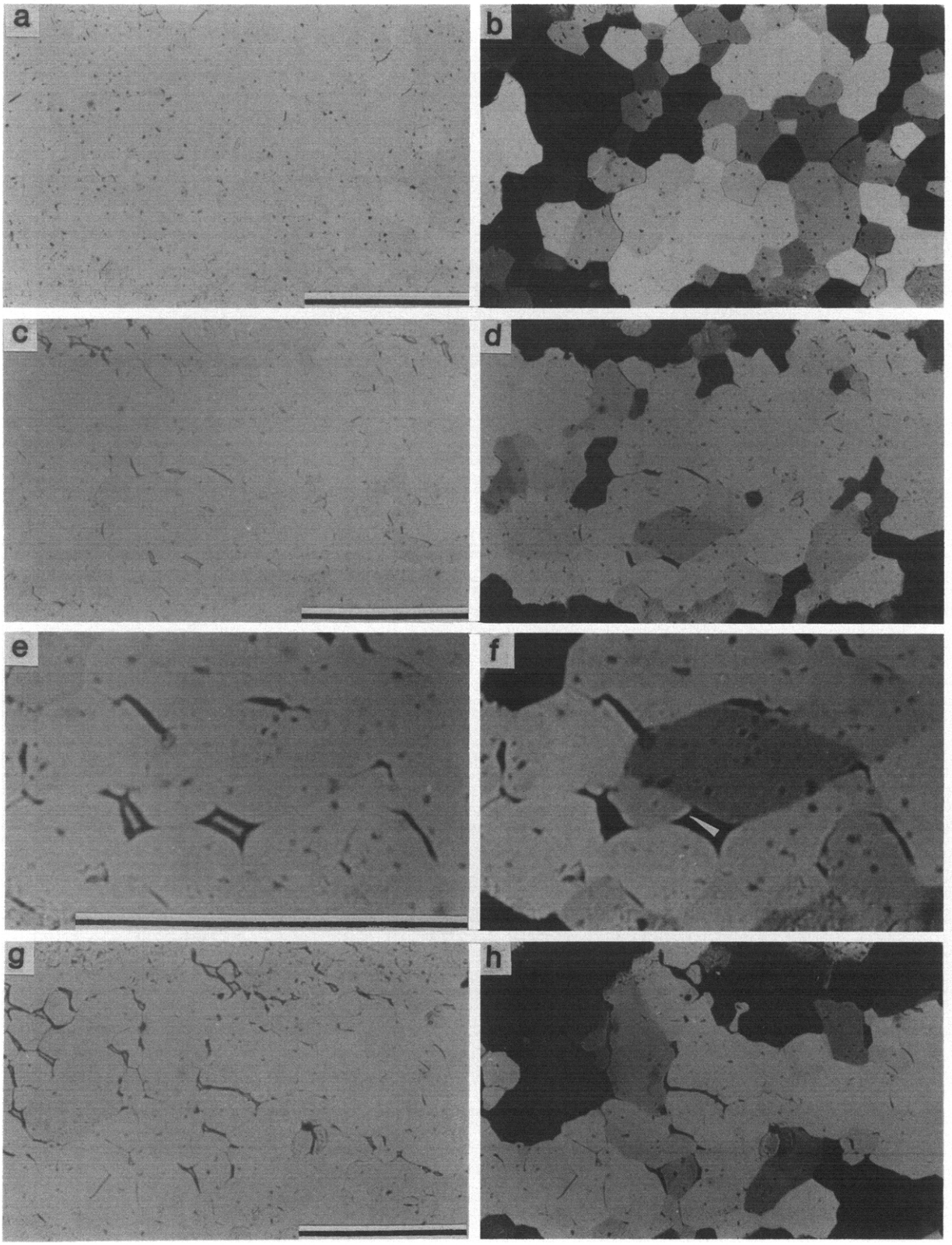

Fig. 7. Plane light and crossed-polars photomicrographs of simple shearing OCP sample TO-105, before deformation (a & b), at $\gamma = 1.1$ (c & d), at $\gamma = 1.2$ (e & f) and immediately after deformation with $\gamma = 1.8$ (g & h). In close-up views (e & f), overgrowth of a grain into the opening (pointer in f) is indicated by a slight difference in interference color of the grain edge adjacent to the opening. Most small black particles are silicon carbide markers. Dextral shear direction is horizontal. Scale bar is 0.5 mm.

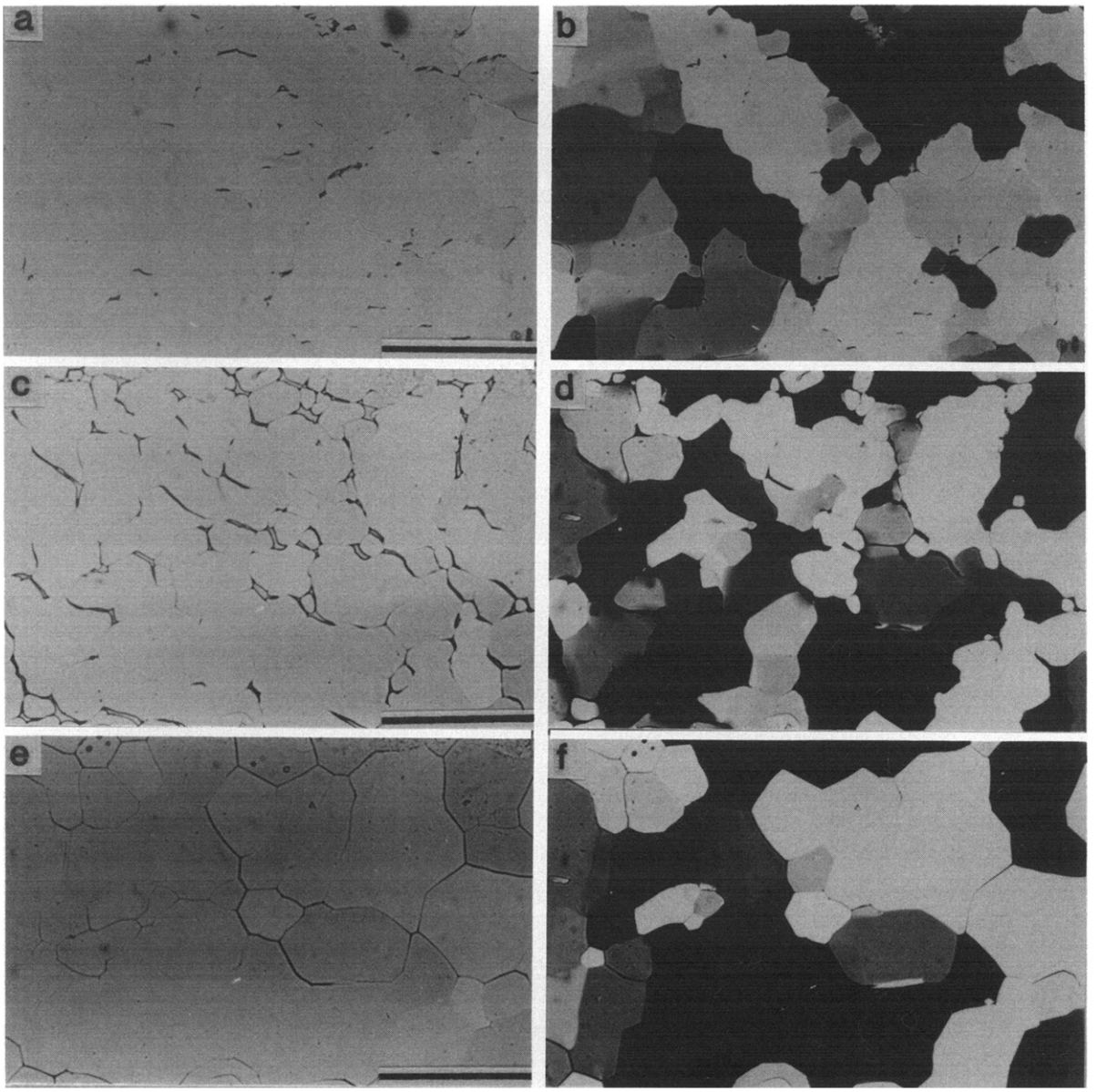

Fig. 8. (a) & (b) Plane light and crossed-polars photomicrographs of pure-shearing OCP sample TO-88 immediately after deformation with about 50% shortening along horizontal direction. (c) & (d) Simple-shearing OCP sample TO-89 immediately after deformation ($\gamma = 1.8$). Dextral shear direction is horizontal. (e) & (f) Same fields as (c) & (d) after 16-h static heating. Scale bar is 0.5 mm.

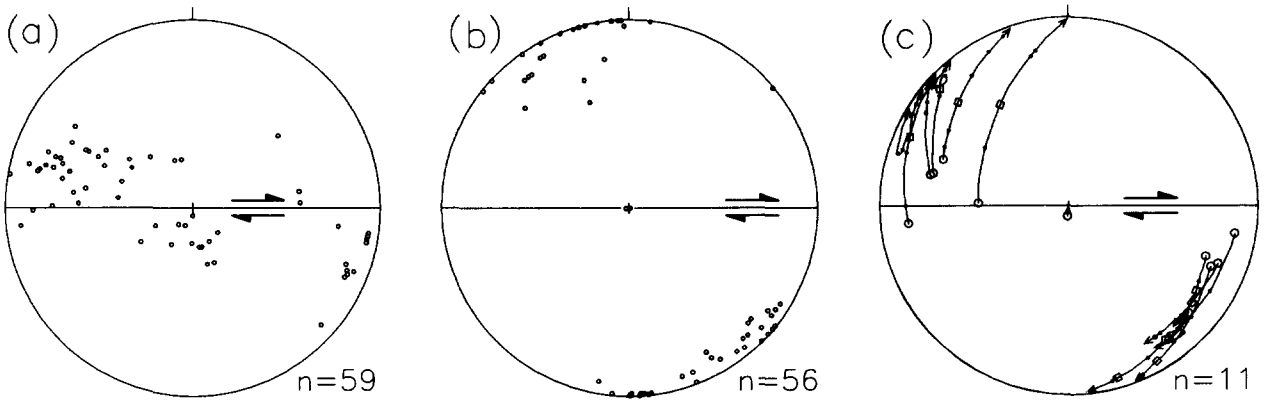

Fig. 9. Lower-hemisphere equal-area projections of *c*-axis of sample TO-105 (a) before and (b) after deformation. (c) *c*-axis reorientation trajectories. Squares represent *c*-axis positions when grain boundary openings begin to occur.

increment of bulk shear strain less than 0.1 (Figs. 12d & e), suggesting the removal of material by diffusion. The upper segment of the boundary between grains 4 and 7 (41 in the earlier stage) moves toward the marker particles in grain 4 as well as toward those in grain 7 (41 in the earlier stage) (Figs. 12a & b). This suggests material efflux from both grains along the boundary. The lower segment of the boundary moves toward the marker particles in grain 4 and away from those in grain 7. The distance of the boundary movement toward the marker particles in grain 4 is larger than that of the boundary movement away from the marker particles in grain 7 (Figs. 12a & b). This may indicate that material efflux from grain 4 occurs together with the conventional volume-conserving grain boundary migration for the lower segment of the boundary. At a possible exten-

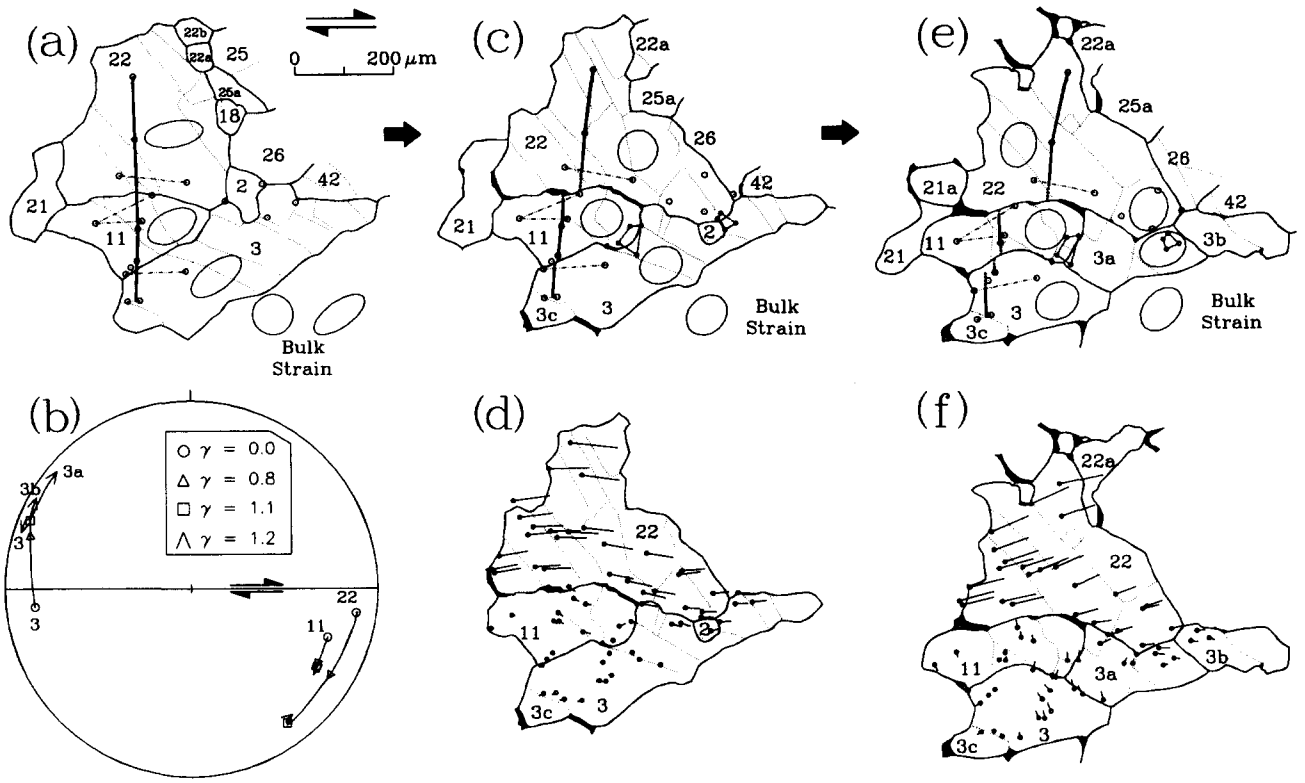

Fig. 10. (a) Map of some grains in sample TO-105. Strains represented by ellipses are strains accumulated from the beginning. Thick line is a material line. Dotted lines are subgrain boundaries. Bulk strain ellipse represents a strain for the total area of the grains shown. Not all marker particles used to calculate strains are shown. (b) *c*-axis trajectories of grains 3, 11 and 22. Grain 3 is recrystallized into three smaller grains later. γs in the inset represent a bulk shear strain of the whole sample. Triangle, square and the tip of arrow correspond to stages (a), (c) and (e), respectively. (c) Offset of the material line by grain boundary sliding. Strain ellipses represent additional strain from (a). Areas outlined by four marker particles at the boundaries between grain 3 and 11, and adjacent to the junction among grains 2, 3 and 22, are indicated by broken lines. (d) Displacements of marker particles which remain in the same grain, relative to a fixed marker particle in grain 11 (solid circle) and the bulk shear direction horizontal. Open circles are positions of marker particles at stage (a) and the other end of strokes are positions at stage (c) or present positions. (e) Further offset of the marker line. Strain ellipses represent additional strains from (a). (f) Displacement of marker particles from stage (c) to (e).

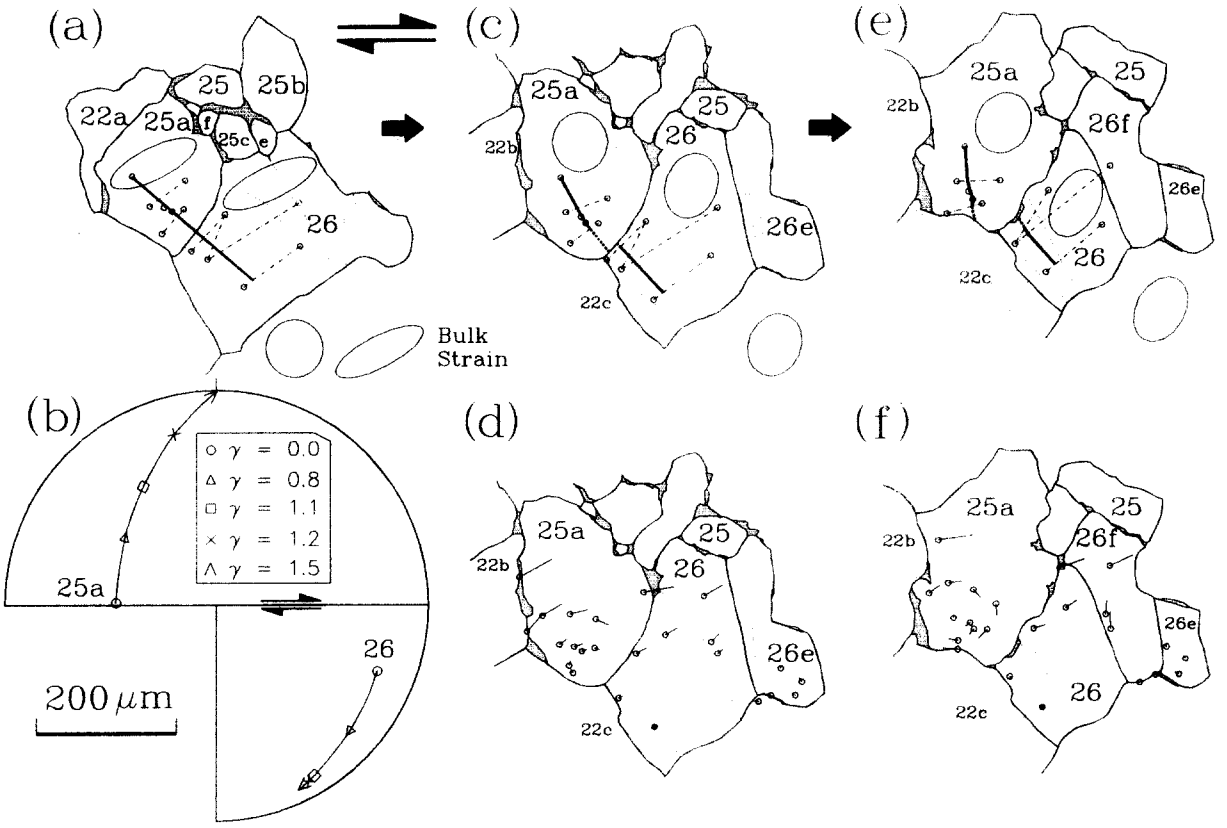

Fig. 11. Offset of a marker line crossing the boundary between grains 25a and 26 in sample TO-105 (a, c & e). Ellipses in (a) indicate strains accumulated from the beginning of deformation. Bulk strain is the strain of the area around grains 25a and 26. Ellipses in (c) & (e) represent additional strains accumulated from (a). (b) *c*-axis trajectories of grains 25a and 26. γ in the inset represents the bulk shear strain of the whole sample. The cross and tips of arrows indicate *c*-axes at stages (a) and (e), respectively. (d) Displacements of marker particles remaining in the same grain from (a) to (c) relative to a fixed marker particle in grain 26 (solid circle) and the bulk shear direction horizontal. (f) Displacements of marker particles from (c) to (e).

sional site (the left boundary of grain 4), the grain boundary opening develops by grain boundary sliding. No loss of the contact between grain 4 and the grain to its left (not shown) along the lower part of the boundary, however, implies that the translation of the grain on the left or diffusional influx may also be involved at this site.

Evolution of grain boundary openings

The experimental results show that openings grow preferentially along grain boundaries at low angles to the shortening direction with grain boundary sliding. Growth of openings usually involves four grains (Figs. 13a & c). Once openings grow, they are shortened parallel to the shortening direction by thrusting of sliding grains and grain overgrowth into the openings. With further deformation they are eventually closed leading to a neighbor switching of four grains (Figs. 13a & c). The magnitude of the minimum principal stretch associated with this neighbor switching is about 0.7. This value is somewhat larger than that (0.58) of Ashby & Verrall's (1973) neighbor switching model where coherency at the boundary is maintained by diffusion without opening. In some cases only two or three grains are involved in the opening and closing of a grain boundary without any neighbor switching (Fig. 13b). Here grain boundary openings are closed as one grain rigidly rotates and the grain boundary bearing the openings becomes perpendicular to the shortening direction.

While grain boundary openings are closed in some places, approximately the same area of grain boundary openings appear in other places. This maintains an approximately steady openings ratio of about 1–3% of the sample volume in simple-shearing experiments and of about 0.5% in pure-shearing experiments without development of any large-scale fracture (Figs. 7, 8 and 14). In one simple-shearing experiment (TO-89), however, the ratio increases by a further 1% toward the end of the deformation. The mean residence time of individual openings corresponds to a shear strain increment of about 0.2 in experiment TO-105 (Ree 1988). Almost all grain boundary openings disappear within 15–20 h if the deformation is stopped but the temperature is maintained (Figs. 8c–f).

In the lowest strain-rate experiment in this group (TO-202), grain boundary openings are closed almost entirely by diffusion. Figure 15 illustrates an example in experiment TO-202 where grain boundary openings grow by grain boundary sliding due to a translation jump between grains (Fig. 15b). The area defined by four marker particles across the boundary between grains 20 and 36 increases by about 20% with the opening of the grain boundary. With further deformation, the opening between grains 20 and 36 becomes closed but the area of

four marker particles shows almost no area change (Figs. 15c & d). As the opening is closed, the northeast boundary of grain 20 and the southwest boundary of grain 36 move away from the marker particles within each grain (Figs. 15b–d). These clearly indicate that the grain boundary opening is healed by diffusional addition of material onto both grain edges adjacent to the opening.

In Fig. 16, the orientations of grain boundary openings at the end of the deformation are shown as rose diagrams with the foliation orientation as a reference horizontal axis. The foliation orientation is defined statistically by the preferred orientation of long axes of grains in this paper. In experiments TO-89 (simple-shearing experiment) and TO-88 (pure-shearing experiment) the openings are preferentially oriented at a high angle to the foliation orientation. Their orientation is also symmetric with respect to the foliation orientation (Figs. 16a & c). In experiment TO-105, however, the preferred orientation of the grain boundary openings is at a low angle to the foliation orientation (Fig. 16b). However in this experiment, the average ratio of long axes to short axes of grains is very low ($\cong 1.05$). With this low value of average grain axial ratio, the definition of foliation orientation is of uncertain significance. In all experiments, the preferred orientation of grain boundary openings is at a high angle to the direction of the maximum finite stretch, and at a low angle to the shortening direction $\dot{S}_3$, assuming $\dot{S}_3$ to be about 45° to the shearing direction in simple shearing experiments and to be parallel to the compression direction in pure shearing experiments (Fig. 16). The orientations of grain boundary openings were also measured at several stages during deformation. They all show more or less constant distribution with respect to the shortening direction as in Fig. 16.

DISCUSSION

Grain boundary sliding, its accommodation and three types of grain boundary migration

As shown in Fig. 1 and several experimental examples, grain boundary sliding is an expression of displacement difference in which material near the contact between grains is brought into the different positions by each domainal deformation of grains. This displacement difference at the contact results from jumps or discontinuities in the strain, rotation and/or translation components of deformation across the boundary. It is known that grain boundary sliding becomes easier as grain boundary cohesion is weakened due to an increase in temperature, decrease in strain rate, and the presence of grain boundary fluid (or melt) films and openings (Marya & Wyon 1975, Mitra 1976, White 1977, Paquet & Francois 1980, Mainprice & Paterson 1984, Weber 1986). The results of experiment TO-105 suggest

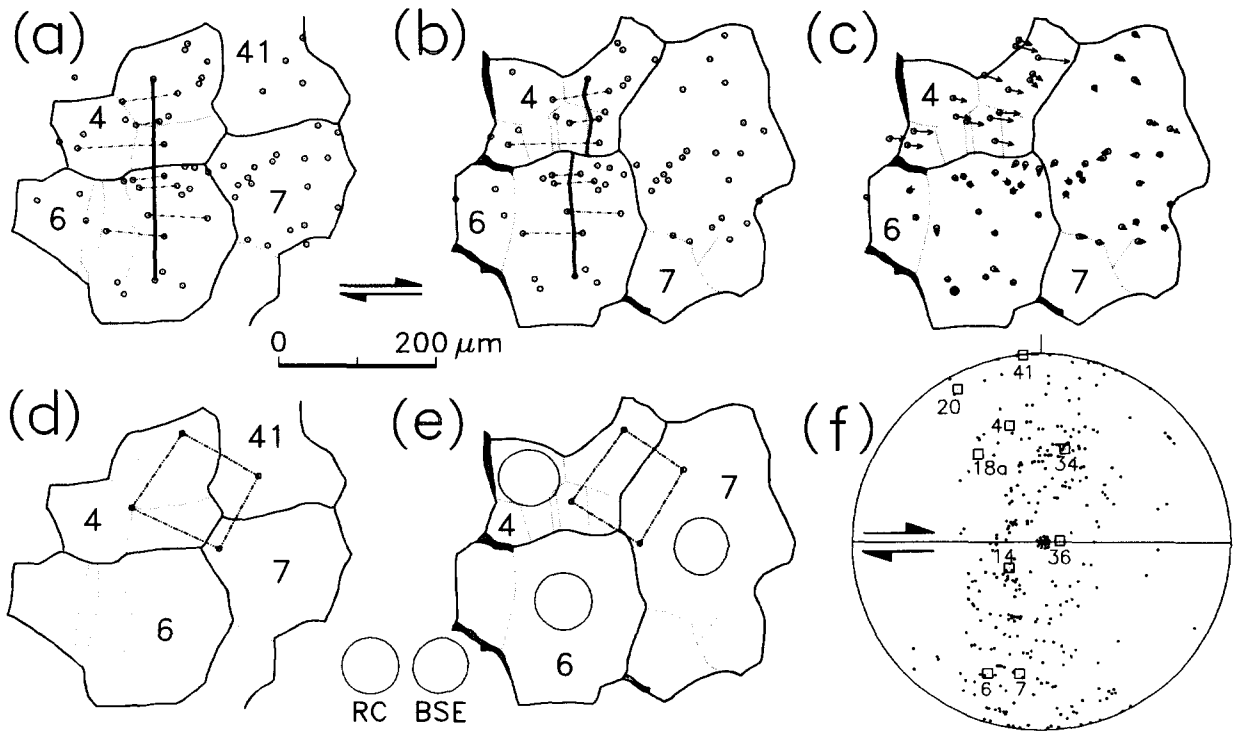

Fig. 12. (a) & (b) Offset of a marker line crossing the boundary between grains 4 and 6 in sample TO-202. (c) Displacements of marker particles remaining in the same grain from (a) to (b), relative to a fixed marker particle in grain 6 (solid circle). The bulk shear direction is horizontal. Duration of deformation in (a) & (b) is 19 and 27 h, respectively. (d) & (e) Change of an area outlined by four marker particles from (a) to (b). Ellipses in (e) indicate strains accumulated from (d). RC, reference circle for strain ellipse. BSE, bulk strain ellipse of the local area around grains 4, 6 and 7. (f) *c*-axis fabric diagram before deformation. *c*-axes of grains shown in Figs. 12 and 15 are numbered and marked as squares. Lower-hemisphere equal-area projection.

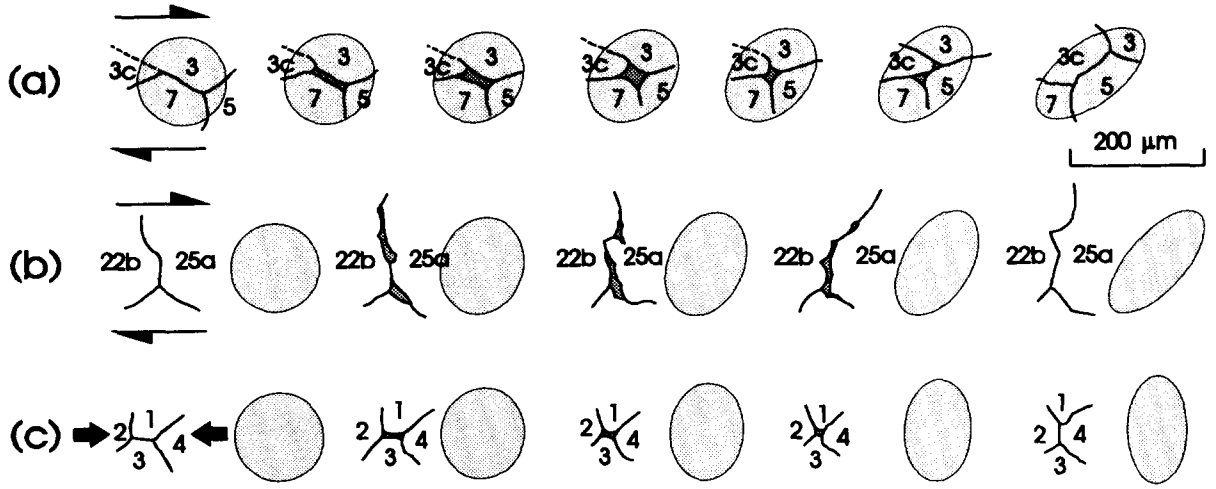

Fig. 13. Opening and closing of grain boundaries in simple-shearing experiment TO-105 (a & b) and pure-shearing experiment TO-100 (c). The bulk shear strains of the whole sample at the start of each sequence of (a) and (b) are about 1.0 and 1.3, respectively. In (c) the start of the sequence corresponds to the beginning of the deformation. Additional strains around grain boundaries or openings are represented by shaded ellipses.

that grain boundary sliding can also be influenced by crystallographic orientation of grains. When many of the grains are unsuitably oriented for single slip on weak systems, grain boundary sliding can be activated in preference to operating other, stronger slip systems.

Among several processes accommodating grain boundary sliding, grain boundary diffusion and intragranular plastic deformation are effective in experimental examples of this paper. The details of accommodation by intragranular plastic deformation are not clear with the present observational scale.

Grain boundary diffusion not only accommodates grain boundary sliding but also results in grain boundary migration. However, diffusion-related grain boundary migration is different from conventional grain boundary migration in being non-conservative, and thus in the details of boundary movement with respect to material points within grains. These grain boundary migrations are classified into three types as follows.

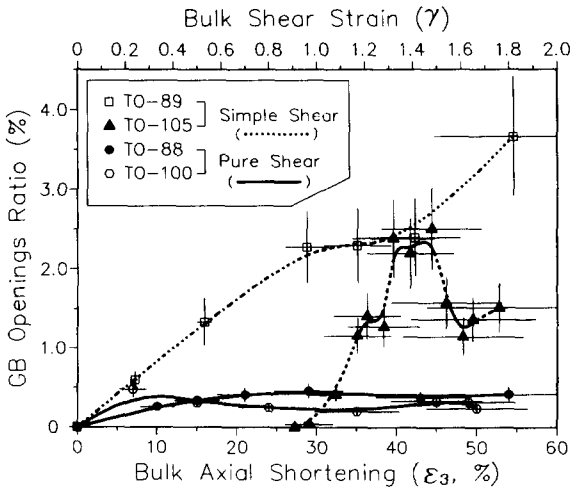

Fig. 14. Plot of bulk strain vs grain boundary openings ratio. Horizontal bars are ± 1 standard deviation of bulk strain. Vertical bars are measurement error ranges of grain boundary openings ratio.

Grain boundary migration (*sensu stricto*) is a movement of a boundary away from material points within one grain and toward material points within the other grain by transferring material across the boundary (Figs. 17a & b) (see also Urai *et al.* 1986). With this process there is no net gain or loss of material in the area swept by the boundary (Type I grain boundary migration).

Grain boundary diffusion, involving a net gain or loss of material, also causes a migration of the grain boundary with respect to material points across the boundary. When material is added to or lost from both grains the boundary will migrate away from or toward the material points, respectively, of both grains (Fig. 17c, Type II grain boundary migration). The upper segment of the boundary between grains 4 and 7 (Figs. 12a & b), and the northeast boundary of grain 20 and southwest boundary of grain 36 (Figs. 15b–d) show Type II migration.

If material is added to or lost from only one grain, the boundary will migrate away from or toward material points, respectively, within that grain whereas it will remain relatively fixed with respect to the material points within the other grain (Fig. 17d, Type III grain boundary migration).

Type I migration can be mixed with Type II or III migration as already seen in the lower segment of the boundary between grains 4 and 7 in Figs. 12(a) & (b). It is also possible that one segment of a boundary may migrate in Type I behavior while the other segment of the boundary migrates in Type II or III fashion.

To investigate the contribution of grain boundary sliding to the total strain, the average axial ratio of intragranular finite strain ellipses ($R_{f,I}$) was compared with the axial ratio of the bulk finite strain ellipse ($R_{f,B}$) in experiments TO-105 and TO-110. In experiment TO-110 where only minor grain boundary openings develop locally, the magnitude of the average intragranular strain ($R_{f,I} = 3.2$) is not much different from that of the bulk strain ($R_{f,B} = 3.3$), suggesting that the contribution of grain boundary sliding to the total strain is minor. In

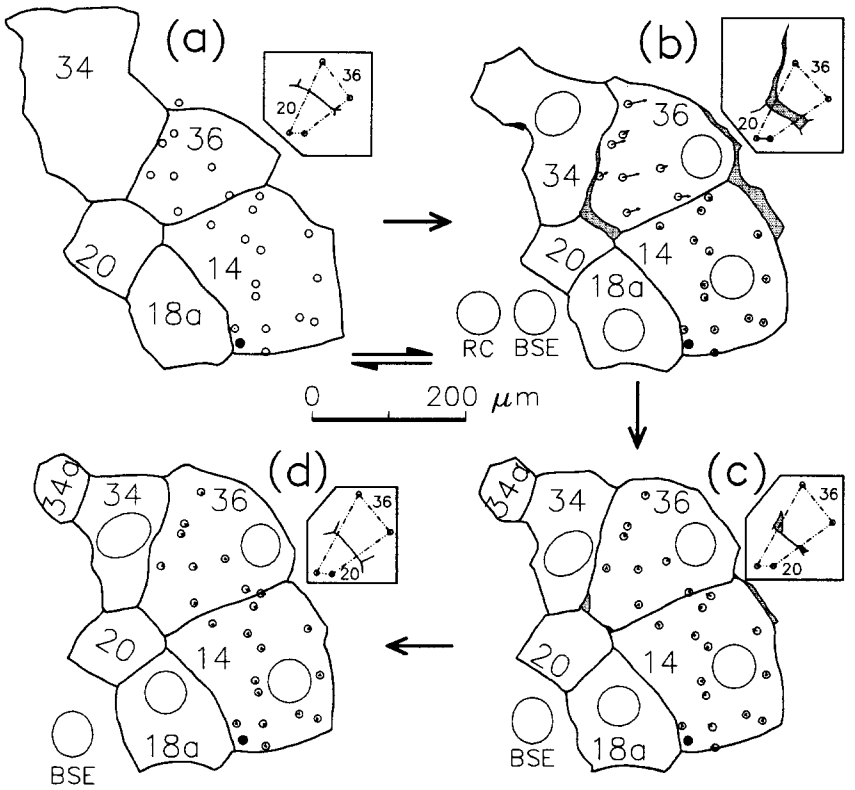

Fig. 15. Opening and closing of grain boundaries in sample TO-202. At stage (a) a small bulk shear strain (less than 0.1) has accumulated since the beginning of deformation. Additional strains accumulated after stage (a) are represented by ellipses in the following sequences (b, c & d). Displacements of marker particles within grains 14 and 36 from a former stage relative to a fixed marker particle in grain 14 (solid circle) are also shown in stages (b), (c) & (d). The inset at the top right of each figure shows change of area outlined by four marker particles around the boundary between grains 20 and 36.

experiment TO-105 where the development of grain boundary openings is relatively extensive, $R_{f,I}$ and $R_{f,B}$ are calculated from when openings begin to occur to the end of the deformation. Here the $R_{f,B}$ value (= 2.3) is larger than the $R_{f,I}$ value (= 1.7). Assuming that grain boundary sliding is the main grain boundary deformation mechanism in this experiment, it accounts for about 25% of the total strain for the above deformation interval.

Implication of grain boundary openings

Grain boundary openings are strongly coupled with grain boundary sliding as explained earlier, and they can also significantly enhance diffusion by providing paths for rapid transport of matter through fluids filling the openings (White & White 1981, Raj 1982). If the growing and closing behavior of grain boundary openings described in this paper operates under natural conditions, fluid will probably circulate preferentially toward growing grain boundary openings and away from closing grain boundary openings. This circulating fluid will shift the sites at which reaction and alteration are concentrated, and will redistribute chemical components (Cox & Etheridge 1989, McCaig & Knipe 1990).

In experimental examples described here, grain boundary openings are closed partly (as in TO-105) or entirely (as in TO-202) by diffusion. However, the diffusion in experiments of this paper may be more

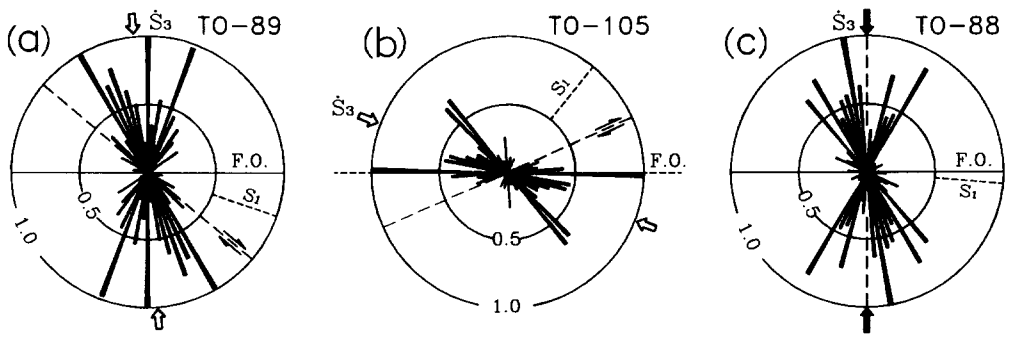

Fig. 16. Rose diagrams of grain boundary openings representing the total length of the long axis per angle of orientation in samples (a) TO-89, (b) TO-105 and (c) TO-88. The length of each orientation (5° interval) is normalized to the maximum length. FO, foliation orientation. S_1, maximum finite stretch direction. $\dot{S}_3$, shortening direction.

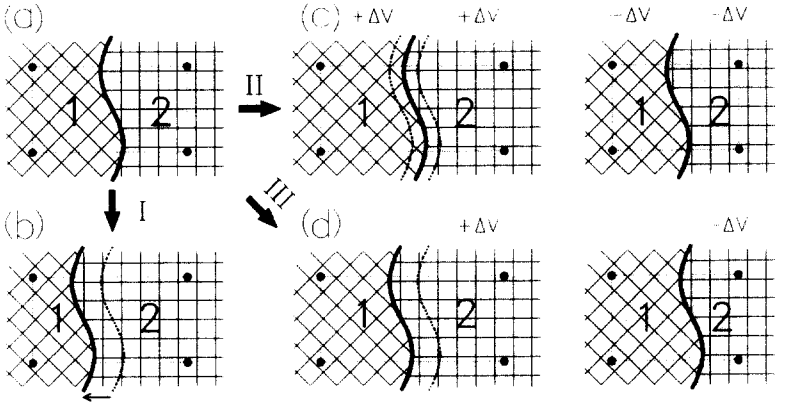

Fig. 17. Schematic representation of the three types of grain boundary migration. Heavy solid lines are grain boundaries. Grids in the grains represent lattice planes. Dots indicate marker particles fixed in the material. (a) Initial state. (b) Type I, (c) Type II, and (d) Type III grain boundary migrations.

efficient than in three-dimensional aggregate samples since there can be an additional pathway for material transport between the glass slides and the sample with the present geometry of experiment.

The preferred alignment of grain boundary openings at low angles to the main shortening direction (S_3) both in pure and simple shearing deformation (Fig. 16) suggests that it may be used as an indicator of the instantaneous stretching or flow stress orientation in situations where older, rotated openings are continuously removed. Of course it is difficult or impossible at present to recognize such situations in naturally deformed materials.

The ratio of grain boundary openings is lower in pure-shearing deformation than in simple-shearing deformation (Fig. 14). This difference may result from the deformation configuration of the present apparatus where a thin sheet of OCP is deformed between two glass slides (see Means 1989, figs. 1c & d). In simple-shearing configuration there exists a tension along the stretching direction whereas there is no tension, only a weaker compression, along the stretching direction in pure-shearing deformation. The presence of tension in the simple-shearing experiments probably facilitates the development of grain boundary openings.

Recognition of grain boundary sliding and opening

White (1977) suggests several potential indicators of grain boundary sliding. These are: constant small grain size; equidimensional grain shape; random lattice orientation; bimodal alignment of grain boundaries; presence of grain boundary bubbles; and presence of high dislocation density adjacent to grain boundary irregularities

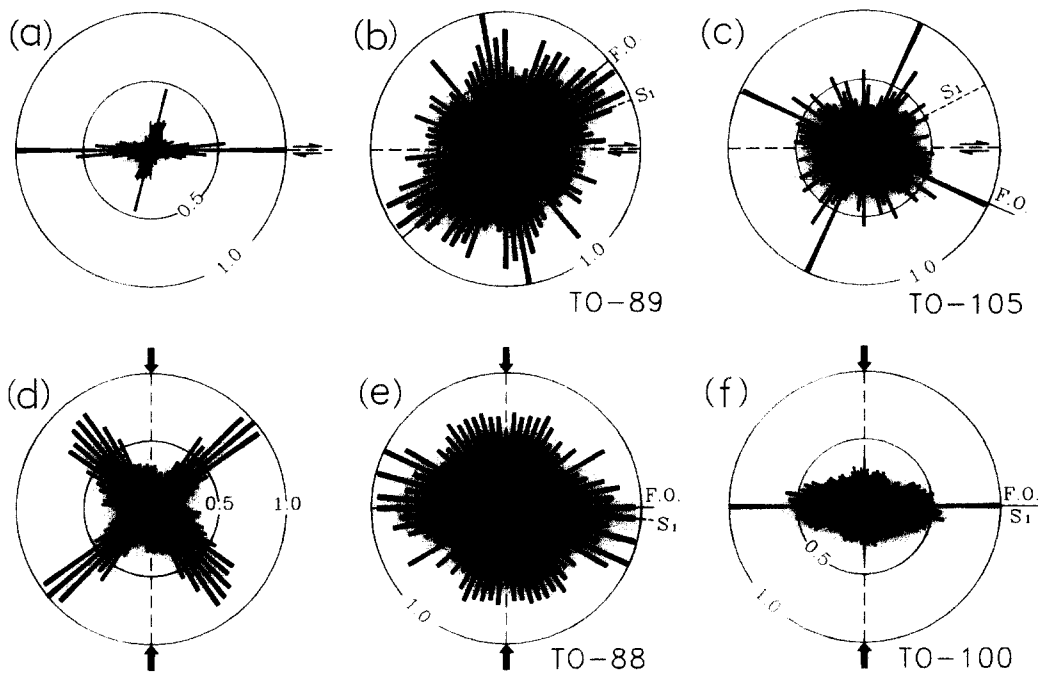

Fig. 18. Rose diagrams of grain boundaries representing the total length of grain boundaries per angle of orientation. (a) & (d) Grain boundary orientations measured from fig. 3 of Drury & Humphreys (1988). (b) & (c) Simple-shearing experiment. (e) & (f) Pure-shearing experiment. FO, foliation orientation. S_1, maximum finite stretch direction.

and triple points. Since the present technique of the experiment described in this paper does not allow the observation of the microstructure on the dislocation scale, the last indicator will not be discussed here.

In experiment TO-105, the average grain area at the end of the deformation is about 1.76×10^{-2} mm^2, which is larger than that of experiment TO-110 ($= 1.23 \times 10^{-2}$ mm^2). Since the grain boundary sliding is more extensive in experiment TO-105, smaller grain size does not necessarily favor grain boundary sliding.

In all experiments where grain boundary sliding appears to be extensive with the development of grain boundary openings, the average grain axial ratio is less than 1.4 throughout the deformation. This value is not much lower than that of experiment TO-110 (about 1.5 from shear strain $\gamma = 0.9$ onwards) where intragranular plastic deformation is more important. Also in another experiment not described here (experiment TO-109), the average grain axial ratio is lower throughout the deformation (1.1–1.3) and intragranular plastic deformation is predominant. Therefore equidimensional grain shape may not be a good indicator of grain boundary sliding.

Random lattice orientation may not be a reliable indicator of grain boundary sliding either since sample TO-105 shows a strong lattice preferred orientation (Fig. 9). It has been suggested that some lattice preferred orientation could develop when grain boundary sliding is accommodated by intracrystalline slip (Edington *et al.* 1976, Etheridge & Wilkie 1979, Schmid *et al.* 1987).

Bimodal alignment of grain boundaries has been considered as a strong evidence of grain boundary sliding (Raj & Ashby 1971, Singh *et al.* 1973, White 1977, Schmid *et al.* 1987, Drury & Humphreys 1988). In simple-shear deformation the first maximum is known to be parallel to the shear zone boundary with the second maximum being at about 70° to the shear zone boundary (Schmid *et al.* 1987, Drury & Humphreys 1988) (Fig. 18a). In pure-shear deformation, two maxima are known to be symmetric with respect to the shortening direction with an angle of about 45° (Singh *et al.* 1973, White 1977, Drury & Humphreys 1988) (Fig. 18d). Although the grain boundary orientation in experiment TO-105 shows two maxima perpendicular to each other, with one maximum 25° off from the bulk shear direction (Fig. 18c), other experiments do not generate a preferred bimodal alignment of grain boundaries (Figs. 18b, e & f).

The preferred orientation of grain boundary openings is seen to be a reliable criterion of grain boundary sliding in experiments described here (Fig. 16). The disappearance of grain boundary openings during static readjustment of the microstructure after deformation (Figs. 8c–f) suggests that it may not be a valuable indicator of grain boundary sliding in naturally deformed rocks. However, if grain boundaries are found to carry remnants of former grain boundary openings such as an array of bubbles or voids and of second-phase inclusions in observation under electron microscopy (White & White 1981, Behrmann 1985), and if these grain boundaries have a well-defined preferred orientation (Behrmann & Mainprice 1987), these will be a strong indicator of the former existence of grain boundary openings and grain boundary sliding. Preferred orientation of grain boundary bands with a slightly different chemical composition from the grain interior (Hall 1984) might be another possible indicator of grain boundary opening and sliding.

SUMMARY

The main contribution of this study has been to present clear evidence of grain boundary sliding, its accommodation processes and the evolution of grain boundary openings. In summary.

(1) Grain boundary sliding reflects discontinuities in the strain, rotation and/or translation components of deformation across the boundary.

(2) Grain boundary sliding can be influenced by a crystallographic preferred orientation of grains. Grains unsuitably oriented for single slip on weak systems contribute to deformation mainly by grain boundary sliding.

(3) Grain boundary diffusion and intragranular plastic deformation accommodate grain boundary sliding.

(4) Grain boundaries migrate in three ways. Type I is conventional, conservative grain boundary migration without any gain or loss of material in the area swept by the boundary. Types II and III are non-conservative grain boundary migrations by grain boundary diffusion involving a net gain or loss of material.

(5) Even when the contribution of grain boundary sliding to the total deformation is minimal (as in TO-110), grain boundary sliding is active from place to place due to local discontinuities of deformation between grains.

(6) When the contribution of grain boundary sliding to the total deformation becomes more important, the development of grain boundary openings is relatively extensive.

(7) These grain boundary openings occur preferentially along grain boundaries at low angles to the shortening direction. Some balance between opening and closing of grain boundaries during deformation maintains an approximately steady openings ratio of about 0.5–3% of a sample area. Almost all grain boundary openings disappear during static readjustment of the microstructure after deformation.

(8) Opening and closing events of grain boundaries during deformation usually involve four grains, leading to a neighbor switching of the grains. The magnitude of the minimum principal stretch associated with this neighbor switching (=0.7) is larger than that (=0.58) of Ashby & Verrall's (1973) switching model.

(9) A well-defined preferred orientation of remnants of former grain boundary openings is a reliable indicator of grain boundary sliding.

Acknowledgements—I am grateful to W. D. Means for his continuous suggestions and encouragement. Discussions with Y.-J. Lee and Y. Park were beneficial. J. A. Gilotti and M. W. Jessell helped to improve an earlier version of the manuscript. Thorough reviews by J. Tullis, J. L. Urai and S. F. Wojtal greatly improved the organization and clarification of this paper, and are appreciated very much. This work was supported by NSF grant EAR 9003954 to W.D. Means.

REFERENCES

Adams, M. A. & Murray, G. T. 1962. Direct observations of grain boundary sliding in bi-crystals of sodium chloride and magnesia. *J. appl. Phys.* **33**, 2126–2131.

Ashby, M. F. & Verrall, R. A. 1973. Diffusion-accommodated flow and superplasticity. *Acta metall.* **21**, 149–163.

Behrmann, J. H. 1985. Crystal plasticity and superplasticity in quartzite; a natural example. *Tectonophysics* **115**, 101–129.

Behrmann, J. H. & Mainprice, D. 1987. Deformation mechanisms in a high-temperature quartz–feldspar mylonite: evidence for superplastic flow in the lower continental crust. *Tectonophysics* **140**, 297–305.

Bons, P. D. & Urai, J. L. 1992. Syndeformational grain growth: microstructures and kinetics. *J. Struct. Geol.* **14**, 1101–1109.

Chokshi, A. H. & Langdon, T. G. 1987. A model for diffusional cavity growth in superplasticity. *Acta metall.* **35**, 1089–1101.

Cox, S. F. & Etheridge, M. A. 1989. Coupled grain-scale dilatancy and mass transfer during deformation. *J. Struct. Geol.* **11**, 142–162.

Crossman, F. W. & Ashby, M. F. 1975. The non-uniform flow of polycrystals by grain-boundary sliding accommodated by power law creep. *Acta metall.* **23**,425–440.

Drury, M. R. & Humphreys, F. J. 1988. Microstructural shear criteria associated with grain boundary sliding during ductile deformation. *J. Struct. Geol.* **10**, 83–89.

Drury, M. R. & Urai, J. L. 1990. Deformation-related recrystallization processes. *Tectonophysics* **172**, 235–253.

Edington, J. W., Melton, K. N. & Cutler, C. P. 1976. Superplasticity. *Prog. Mater. Sci.* **21**, 63–170.

Edward, G. H. & Ashby, M. F. 1979. Intergranular fracture during power-law creep. *Acta metall.* **27**, 1505–1518.

Etheridge, M. A. & Wilkie, J. C. 1979. Grain size reduction, grain boundary sliding and the flow strength of mylonites. *Tectonophysics* **58**, 159–178.

Gifkins, R. C. 1976. Grain-boundary sliding and its accommodation during creep and superplasticity. *Met. Trans.* **7A**, 1225–1232.

Hall, P. C. 1984. Some aspects of deformation fabrics along the Highland/Lowland boundary, northwest Adirondacks, New York State. Unpublished M. S. thesis, State University of New York at Albany.

Hashimoto, S., Fujii, T. K. & Miura, S. 1987. Grain-boundary sliding and triple-point fold in aluminium tricrystals. *Scr. Met.* **21**, 169–174.

Knipe, R. J. 1989. Deformation mechanisms—recognition from natural tectonites. *J. Struct. Geol.* **11**, 127–146.

Langdon, T. G. 1970. Grain boundary sliding as a deformation mechanism during creep. *Phil. Mag.* **22**, 689–700.

Langdon, T. G. 1975. Grain boundary deformation processes. In: *Deformation of Ceramic Materials* (edited by Bradt, R. C. & Tressler, R. E.). Plenum, New York, 101–126.

Langdon, T. G. 1981. Deformation of polycrystalline materials at high temperatures. In: *Deformation of Polycrystals: Mechanisms and Microstructures* (edited by Hansen, N., Horsewell, A., Leffers, T. & Lilholt, H.). Risø Nat. Lab., Roskilde, Denmark, 45–54.

Langdon, T. G. & Vastava, R. B. 1982. An evaluation of deformation models for grain boundary sliding. In: *Mechanical Testing for Deformation Model Development* (edited by Rohde, R. W. & Swearengen, J. C.). American Society for Testing materials, Philadelphia, 435–451.

Marya, S. K. & Wyon, G. 1975. Superplasticité a l'ambiante de l'aluminium a grain fin, en liaison avec l'existence d'un film intergranulaire de solution solide riche en gallium. *J. Physique* **36**, 309–313.

Mainprice, D. H. & Paterson, M. S. 1984. Experimental studies of the role of water in the plasticity of quartzite. *J. geophys. Res.* **89**, 4257–4296.

McCaig, A. M. & Knipe, R. J. 1990. Mass-transport mechanism in deforming rocks: recognition using microstructural and microchemical data. *Geology* **18**, 824–827.

Means, W. D. 1989. Synkinematic microscopy of transparent polycrystals. *J. Struct. Geol.* **11**, 163–174.

Means, W. D. & Jessell, M. W. 1986. Accommodation migration of grain boundaries. *Tectonophysics* **127**, 67–86.

Means, W. D. & Ree, J.-H. 1990. Structural motion, particle motion, and migration processes in deforming materials. *Geol. Soc. Am. Abs. w. Prog.* **22**, A138.

Mitra, S. 1976. A quantitative study of deformation mechanisms and finite strain in quartzites. *Contr. Miner. Petrol.* **59**, 203–226.

Naziri, H., Pearce, R., Henderson-Brown, M. & Hale, K. F. 1973. *In situ* superplasticity experiment in the 1 million volt electron microscope. *J. Microsc.* **97**, 229–238.

Naziri, H., Pearce, R., Henderson-Brown, M. & Hale, K. F. 1975. Microstructural–mechanism relationship in the zinc-aluminium eutectoid superplastic alloy. *Acta metall.* **23**, 489–496.

Paquet, J. & Francois, P. 1980. Experimental deformation of partially melted granitic rock at 600–900°C and 250 MPa confining pressure. *Tectonophysics* **68**, 131–146.

Poirier, J.-P. 1985. *Creep of Crystals*. Cambridge University Press, Cambridge.

Raj, R. 1982. Creep in polycrystalline aggregates by matter transport through a liquid phase. *J. geophys. Res.* **87**, 4731–4739.

Raj, R. & Ashby, M. F. 1971. On grain boundary sliding and diffusional creep. *Met. Trans.* **2**, 1113–1127.

Ree, J.-H. 1988. Evolution of deformation-induced grain boundary voids in octachloropropane. *Geol. Soc. Am. Abs. w. Prog.* **20**, A213.

Ree, J.-H. 1990. High temperature deformation of octachloropropane: dynamic grain growth and lattice reorientation. In: *Deformation Mechanisms, Rheology and Tectonics* (edited by Knipe, R. J. & Rutter, E. H.). *Spec. Publs geol. Soc. Lond.* **54**, 363–368.

Ree, J.-H. 1991. An experimental steady-state foliation. *J. Struct. Geol.* **13**, 1001–1011.

Schmid, S. M. 1982. Microfabric studies as indicators of deformation mechanisms and flow laws operative in mountain building. In: *Mountain Building Processes* (edited by Hsü, K. J.). Academic Press, London, 95–110.

Schmid, S. M., Boland, J. N. & Paterson, M. S. 1977. Superplastic flow in fine-grained limestone. *Tectonophysics* **43**, 257–291.

Schmid, S. M., Panozzo, R. & Bauer, S. 1987. Simple shear experiments on calcite rocks: rheology and microfabric. *J. Struct. Geol.* **9**, 747–778.

Singh, V. Rao, P. & Taplin, D. M. R. 1973. On the role of grain boundary migration during the creep of zinc. *J. Mater. Sci.* **8**, 373–381.

Speight, M. V. 1976. The role of grain-boundary sliding in the creep of polycrystals. *Acta metall.* **24**, 725–729.

Stowell, M. J., Livesey, D. W. & Ridley, N. 1984. Cavity coalescence in superplastic deformation. *Acta metall.* **32**, 35–42.

Urai, J. L., Means, W. D. & Lister, G. S. 1986. Dynamic recrystallization of minerals. In: *Mineral and Rock Deformation: Laboratory Studies—The Paterson Volume* (edited by Heard, H. C. & Hobbs, B. E.). *Am. Geophys. Un. Geophys. Monogr.* **36**, 161–199.

Weber, K. 1986. Metamorphism and crustal rheology—implications for the structural development of the continental crust during prograde metamorphism. In: *The Nature of the Lower Continental Crust* (edited by Dawson, J. B., Carswell, D. A., Hall, J. & Wedepohl, K. H.). *Spec. Publs geol. Soc. Lond.* **24**, 95–106.

White, J. C. & White, S. H. 1981. On the structure of grain boundaries in tectonites. *Tectonophysics* **78**, 613–628.

White, S. 1977. Geological significance of recovery and recrystallization processes in quartz. *Tectonophysics* **39**, 143–170.

Zeuch, D. H. 1984. Application of a model for grain boundary sliding to high temperature flow of Carrara Marble. *Mech. Mater.* **3**, 111–117.